

# 1 Nitrogen Fixation in Arctic Coastal Waters (Qeqertarsuaq, West 2 Greenland): Influence of Glacial Melt on Diazotrophs, Nutrient 3 Availability, and Seasonal Blooms

4 Schlangen Isabell<sup>1</sup>, Leon-Palmero Elizabeth<sup>1,2</sup>, Moser Annabell<sup>1</sup>, Xu Peihang<sup>1</sup>, Laursen Erik<sup>1</sup>, and  
5 Löscher Carolin R.<sup>1,3</sup>

6 <sup>1</sup>Nordceee, Department of Biology, University of Southern Denmark, Campusvej 55, 5230 Odense M, Denmark

7 <sup>2</sup>Department of Geosciences, Princeton University, Princeton, New Jersey

8 <sup>3</sup>DIAS, University of Southern Denmark, Odense, Denmark

9 **Correspondence:** Carolin R. Löscher (cloescher@biology.sdu.dk)

10  
11 **Abstract.** The Arctic Ocean is undergoing rapid transformation due to climate change, with decreasing sea ice contributing  
12 to a predicted increase in primary productivity. A critical factor determining future productivity in this region is the  
13 availability of nitrogen, a key nutrient that often limits biological growth in Arctic waters. The fixation of dinitrogen (N<sub>2</sub>)  
14 gas, a biological process mediated by diazotrophs, not only supplies new nitrogen to the ecosystem but also plays a  
15 central role in shaping the biological productivity of the Arctic. Historically it was believed to be limited to oligotrophic  
16 tropical and subtropical oceans, Arctic N<sub>2</sub> fixation has only garnered significant attention over the past decade, leaving  
17 a gap in our understanding of its magnitude, the diazotrophic community, and potential environmental drivers. In this  
18 study, we investigated N<sub>2</sub> fixation rates and the diazotrophic community in Arctic coastal waters, using a combination of  
19 isotope labeling, genetic analyses and biogeochemical profiling, in order to explore its response to glacial meltwater,  
20 nutrient availability and its impact on primary productivity. Here we show N<sub>2</sub> fixation rates ranging from 0.16 to 2.71 nmol  
21 N L<sup>-1</sup> d<sup>-1</sup>, to be notably higher than those observed in many other oceanic regions, suggesting a previously unrecognized  
22 significance of N<sub>2</sub> fixation in these high-latitude waters. The diazotrophic community is predominantly composed of  
23 UCYN-A. We found highest N<sub>2</sub> fixation rates co-occurring with maximum chlorophyll *a* concentrations and primary  
24 production rates at a station in the Vaigat Strait close impacted by glacier meltwater inflow, possibly providing otherwise  
25 limiting nutrients. Our findings illustrate the importance of N<sub>2</sub> fixation in an environment previously not considered  
26 important for this process and provide insights into its response to the projected melting of the polar ice cover.

## 27 28 1 Introduction

29  
30 Nitrogen is a key element for life and often acts as a growth-limiting factor for primary productivity (Gruber and Sarmiento,  
31 1997; Gruber, 2004; Gruber and Galloway, 2008). Despite nitrogen gas (N<sub>2</sub>) making up approximately 78% of the  
32 atmosphere, it remains inaccessible to most marine life forms. Diazotrophs, which are specialized bacteria and archaea,  
33 have the ability to convert N<sub>2</sub> into biologically available nitrogen, facilitated by the nitrogenase enzyme complex carrying  
34 out the process of

35 biological nitrogen fixation ( $N_2$  fixation) (Capone and Carpenter (1982)). Despite the fact that these organisms are highly  
36 specialized and  $N_2$  fixation is energetically demanding, the ability to carry out this process is widespread amongst  
37 prokaryotes. However, it is controlled by several factors such as temperature, light, nutrients and trace metals such as iron  
38 and molybdenum (Sohm et al., 2011; Tang et al., 2019). Oceanic  $N_2$  fixation is the major source of nitrogen to the marine  
39 system (Karl et al., 2002; Gruber and Sarmiento, 1997), thus, diazotrophs determine the biological productivity of our  
40 planet (Falkowski et al. (2008), impact the global carbon cycle and the formation of organic matter (Galloway et al., 2004;  
41 Zehr and Capone, 2020). Traditionally it has been believed that the distribution of diazotrophs was limited to warm and  
42 oligotrophic waters (Buchanan et al., 2019; Sohm et al., 2011; Luo et al., 2012) until putative diazotrophs were identified  
43 in the central Arctic Ocean and Baffin Bay (Farnelid et al., 2011; Damm et al., 2010). First rate measurements have been  
44 reported for the Canadian Arctic by Blais et al. (2012) and recent studies have reported rate measurements in adjacent seas  
45 (Harding et al., 2018; Sipler et al., 2017; Shiozaki et al., 2017, 2018), drawing attention to cold and temperate waters as  
46 significant contributors to the global nitrogen budget through diverse organisms.

47  $N_2$  fixation is performed by diverse group of cyanobacteria as well as by non-cyanobacteria diazotrophs (NCDs). UCYN-  
48 A has been described as the dominant active  $N_2$  fixing cyanobacterial diazotroph in arctic waters (Harding et al. (2018)),  
49 while other cyanobacteria have only occasionally been reported (Díez et al., 2012; Fernández-Méndez et al., 2016; Blais et  
50 al., 2012). Recent studies found that the majority of the arctic marine diazotrophs are NCDs and those may contribute  
51 significantly to  $N_2$  fixation in the Arctic Ocean (Shiozaki et al., 2018; Fernández-Méndez et al., 2016; Harding et al., 2018;  
52 Von Friesen and Rie- mann, 2020). Still, studies on the Arctic diazotroph community remain scarce, leaving Arctic  
53 environments poorly understood regarding  $N_2$  fixation. Shao et al. (2023) note the impossibility of estimating Arctic  $N_2$   
54 fixation rates due to the sparse spatial coverage, which currently represents only approximately 1 % of the Arctic Ocean.  
55 Increasing data coverage in future studies will aid in better constraining the contribution of  $N_2$  fixation to the global oceanic  
56 nitrogen budget (Tang et al. (2019)).

57 The Arctic ecosystem is undergoing significant changes driven by rising temperatures and the accelerated melting of sea ice,  
58 a trend predicted to intensify in the future (Arrigo et al., 2008; Hanna et al., 2008; Haine et al., 2015). These climate-driven  
59 shifts have stimulated primary productivity in the Arctic by 57 % from 1998 to 2018, elevating nutrient demands in the  
60 Arctic Ocean (Ardyna and Arrigo, 2020; Arrigo and van Dijken, 2015; Lewis et al., 2020). This increase is attributed to  
61 prolonged phytoplankton growing seasons and expanding ice-free areas suitable for phytoplankton growth (Arrigo et al.  
62 (2008)). However, despite these dramatic changes, the role of  $N_2$  fixation in sustaining Arctic primary production remains  
63 poorly understood. While recent studies suggest that diazotrophic activity may contribute to nitrogen inputs in polar regions  
64 (Sipler et al. (2017)), fundamental uncertainties remain regarding the extend, distribution and environmental drivers of  $N_2$   
65 Fixation in the Arctic Ocean. Specifically, it is unclear whether increased glacial meltwater input enhances or inhibits  $N_2$   
66 Fixation through changes in nutrient availability, stratification, and microbial community composition. Thus, the question  
67 of whether nitrogen limitation will emerge as a key factor constraining Arctic primary production under future climate scenarios  
68 remains unresolved. In this study, we investigate the diversity of diazotrophic communities alongside in situ  $N_2$  fixation

rate measurements in Disko Bay (Qeqertarsuaq), a coastal Arctic system strongly influenced by glacial meltwater input. By linking environmental parameters to N<sub>2</sub> fixation dynamics, we aim to clarify the role of diazotrophs in Arctic nutrient cycling and assess their potential contribution to sustaining primary production in a changing Arctic. Understanding these processes is essential for refining biogeochemical models and predicting ecosystem responses to future climate change.

## 73 74     2 Material and methods

### 75     76     2.1 Seawater sampling

77     78     The research expedition was conducted from August 16 to 26 in 2022 aboard the Danish military vessel P540 within the  
79     waters of Qeqertarsuaq, located in the western region of Greenland (Kalaallit Nunaat). Discrete water samples were  
80     obtained using a 10 L Niskin bottle, manually lowered with a hand winch to five distinct depths (surface, 5, 25, 50, and  
81     100 m). A comprehensive sampling strategy was employed at 10 stations (Fig. 1), covering the surface to a depth of 100 m.  
82     The sampled parameters included water characteristics, such as nutrient concentrations, chl *a*, particulate organic carbon  
83     (POC) and nitrogen (PON), molecular samples for nucleic acid extractions (DNA), dissolved inorganic carbon (DIC) as  
84     well as CTD sensor data. At three selected stations (3,7,10) N<sub>2</sub> fixation and primary production rates were quantified  
85     through concurrent incubation experiments.

86     87     Samples for nutrient analysis, nitrate (NO<sub>3</sub><sup>-</sup>), nitrite (NO<sub>2</sub><sup>-</sup>) and phosphate (PO<sub>4</sub><sup>3-</sup>) were taken in triplicates, filtered  
88     through a 0.22  $\mu$ m syringe filter (Avantor VWR® Radnor, Pa, USA) and stored at -20 °C until further analysis.  
89     Concentrations were spectrophotometrically determined (Thermo Scientific, Genesys 1OS UV-VIS spectrophotometer)  
90     following the established protocols of Murphy and Riley (1962) for PO<sub>4</sub><sup>3-</sup>; García-Robledo et al. (2014) for NO<sub>3</sub><sup>-</sup> & NO<sub>2</sub><sup>-</sup>  
91     (detection limits: 0.01  $\mu$ mol L<sup>-1</sup> (NO<sub>3</sub><sup>-</sup>, NO<sub>2</sub><sup>-</sup>, and PO<sub>4</sub><sup>3-</sup>), 0.05  $\mu$ mol L<sup>-1</sup> (NH<sub>4</sub><sup>+</sup>)). Chl *a* samples were filtered onto 47 mm  
92     ø GF/F filters (GE Healthcare Life Sciences, Whatman, USA), placed into darkened 15 mL LightSafe centrifuge tubes  
93     (Merck, Rahway, NJ, USA) and were subsequently stored at -20 °C until further analysis. To determine the Chl *a* con-  
94     centration, the samples were immersed in 8 mL of 90 % acetone overnight at 5 °C. Subsequently, 1 mL of the resulting  
95     solution was transferred to a 1.5 mL glass vial (Mikrolab Aarhus A/S, Aarhus, Denmark) the following day and subjected  
96     to analysis using the Trilogy® Fluorometer (Model #7200-00) equipped with a Chl *a* in vivo blue module (Model #7200-  
97     043, both Turner Designs, San Jose, CA, USA). Measurements of serial dilutions from a 4 mg L<sup>-1</sup> stock standard and 90 %  
98     acetone (serving as blank) were performed to calibrate the instrument. In addition, measurements of a solid-state secondary  
99     standard were performed every 10 samples. Water (1 L) water from each depth was filtered for the determination of POC  
100     and PON concentrations, as well as natural isotope abundance ( $\delta$  <sup>13</sup>C POC /  $\delta$  <sup>15</sup>N PON) using 47 mm ø, 0.7  $\mu$ m nominal  
101     pore size precombusted GF/F filter (GE Healthcare Life Sciences, Whatman, USA), which were subsequently stored at -  
102     20 °C until further analysis. Seawater samples for DNA were filtered through 47 mm ø, 0.22  $\mu$ m MCE membrane filter  
103     (Merck, Millipore Ltd., Ireland) for a maximum of 20 minutes, employing a gentle vacuum (200 mbar). The filtered  
volumes varied depending

104 on the amount of material captured on the filter, ranging from 1.3 L to 2 L, with precise measurements recorded. The filters  
105 were promptly stored at -20 °C on the ship and moved to -80 °C upon arrival to the lab until further analysis.

106 To achieve detailed vertical profiles, a conductivity-temperature-depth-profiler (CTD, Seabird X) equipped with  
107 supplementary sensors for dissolved oxygen (DO), photosynthetic active radiation (PAR), and fluorescence (Fluorometer)  
108 was manually deployed.

109 **2.2 Nitrogen fixation and primary production**

110 Water samples were collected at three distinct depths (0, 25 and 50 m) for the investigation of N<sub>2</sub> fixation rates and primary  
111 production rates, encompassing the euphotic zone, chlorophyll maximum, and a light-absent zone. Three incubation  
112 stations (Fig. 2: station 3, 7, 10) were chosen, in a way to cover the variability of the study area. This strategic sampling  
113 aimed to capture a gradient of the water column with varying environmental conditions, relevant to the aim of the study.  
114 N<sub>2</sub> fixation rates were assessed through triplicate incubations employing the modified <sup>15</sup>N-N<sub>2</sub> dissolution technique after  
115 Großkopf et al. (2012) and Mohr et al. (2010).

116 To ensure minimal contamination, 2.3 L glass bottles (Schott-Duran, Wertheim, Germany) underwent pre-cleaning and  
117 acid washing before being filled with seawater samples. Oxygen contamination during sample collection was mitigated by  
118 gently and bubble-free filling the bottles from the bottom, allowing the water to overflow. Each incubation bottle received  
119 a 100 mL amendment of <sup>15</sup>N-N<sub>2</sub> enriched seawater (98 %, Cambridge Isotope Laboratories, Inc., USA) achieving an  
120 average dissolved N<sub>2</sub> isotope abundance (<sup>15</sup>N atom %) of  $3.90 \pm 0.02$  atom % (mean  $\pm$  SD). Additionally, 1 mL of  $H^{13}CO_3$   
121 (1g/50 mL) (Sigma- Aldrich, Saint Louis Missouri US) was added to each incubation bottle, roughly corresponding to 10  
122 atom % enrichment and thus measurements of primary production and N<sub>2</sub> fixation were conducted in the same bottle.  
123 Following the addition of both isotopic components, the bottles were closed airtight with septa-fitted caps and incubated for  
124 24 hours on-deck incubators with a continuous surface seawater flow. These incubators, partially shaded (using daylight-  
125 filtering foil) to simulate in situ photosynthetically active radiation (PAR) conditions, aimed to replicate environmental  
126 parameters experienced at the sampled depths. Control incubations utilizing atmospheric air served as controls to monitor  
127 any natural changes in  $\delta^{15}N$  not attributable to <sup>15</sup>N-N<sub>2</sub> addition. These control incubations were conducted using the  
128 dissolution method, like the <sup>15</sup>N-N<sub>2</sub> enrichment experiments, but with the substitution of atmospheric air instead of isotopic  
129 tracer.

130 After the incubation period, subsamples for nutrient analysis were taken from each incubation sample, and the remaining  
131 content was subjected to the filtration process and were gently filtered (200 mbar) onto precombusted GF/F filters  
132 (Advantec,

133 47 mm ø, 0.7  $\mu$ m nominal pore size). This step ensured a comprehensive examination of both nutrient dynamics and the  
134 isotopic composition of the particulate pool in the incubated samples. Samples were stored at -20 °C until further analysis.  
135 Upon arrival in the lab, the filters were dried at 60 °C and to eliminate particulate inorganic carbon, subsequently subject  
136 to acid fuming during which they were exposed to concentrated hydrochloric acid (HCl) vapors overnight in a desiccator.

138 After undergoing acid treatment, the filters were carefully dried, then placed into tin capsules and pelletized for subsequent  
139 analysis. The determination of POC and PON, as well as isotopic composition ( $\delta^{13}\text{C}$  POC /  $\delta^{15}\text{N}$  PON), was carried out  
140 using an elemental analyzer (Flash EA, ThermoFisher, USA) connected to a mass spectrometer (Delta V Advantage Isotope  
141 Ratio MS, ThermoFisher, USA) with the ConFlo IV interface. This analytical setup was applied to all filters. These values,  
142 derived from triplicate incubation measurements, exhibited no omission of data points or identification of outliers. Final rate  
143 calculations for  $\text{N}_2$  fixation rates were performed after Mohr et al. (2010) and primary production rates after Slawyk et al.  
144 (1977).

### 145 2.3 Molecular methods

146  
147 The filters were flash-frozen in liquid nitrogen, crushed and DNA was extracted using the Qiagen DNA/RNA AllPrep Kit  
148 (Qi- agen, Hildesheim, DE), following the procedure outlined by the manufacturer. The concentration and quality of the  
149 extracted DNA was assessed spectrophotometrically using a MySpec spectrofluorometer (VWR, Darmstadt, Germany).  
150 The prepara- tion of the metagenome library and sequencing were performed by BGI (China). Sequencing libraries were  
151 generated using MGIEasy Fast FS DNA Library Prep Set following the manufacturer's protocol. Sequencing was  
152 conducted with 2x150bp on a DNBSEQ-G400 platform (MGI). SOAPnuke1.5.5 (Chen et al. (2018)) was used to filter  
153 and trim low quality reads and adaptor contaminants from the raw sequence reads, as clean reads. In total, fifteen  
154 metagenomic datasets were produced with an average of 9.6G bp per sample.

#### 155 2.3.1 Metagenomic De Novo assembly, gene prediction, and annotation

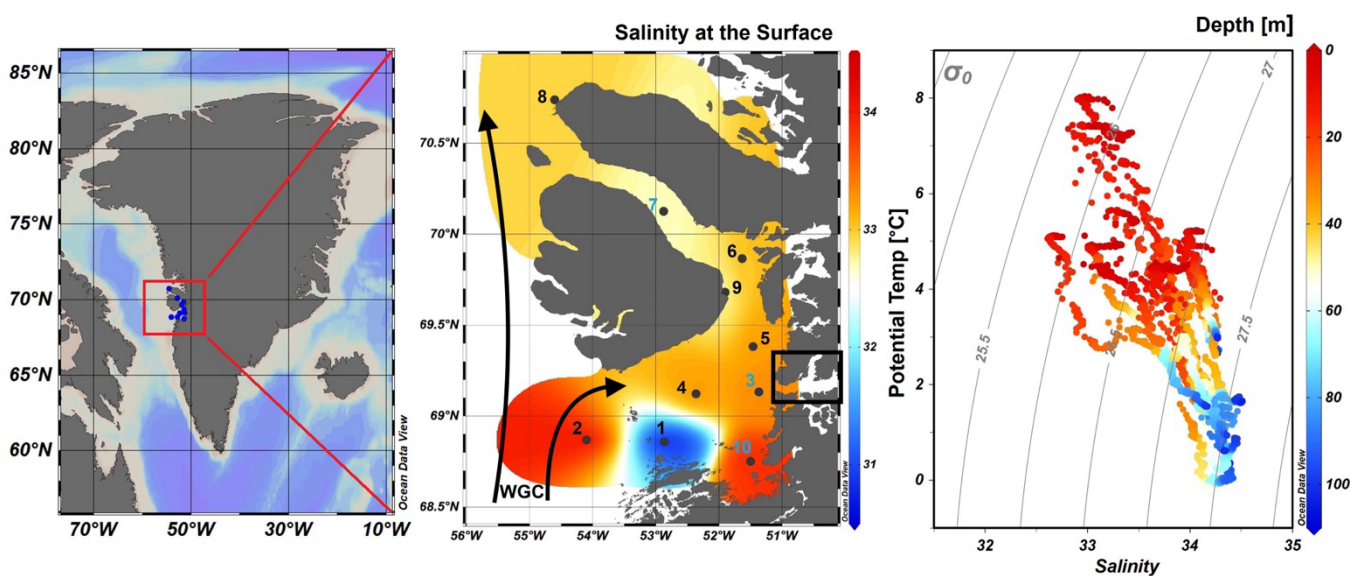
156  
157 Megahit v1.2.9 (Li et al. (2015)) was used to assemble clean reads for each dataset with its minimum contig length as 500.  
158 Prodigal v2.6.3 (Hyatt et al. (2010)) with the setting of “-p meta” was then used to predict the open reading frames (ORFs)  
159 of the assembled contigs. ORFs from all the available datasets were filtered (>100bp), dereplicated and merged into a  
160 catalog of non-redundant genes using cd-hit-est (>95 % sequence identity) (Fu et al. (2012)). Salmon v1.10.0 (Patro et al.  
161 (2017)) with the “– meta” option was employed to map clean reads of each dataset to the catalog of non-redundant genes  
162 and generate the GPM (genes per million reads) abundance. EggNOG mapper v2.1.12 (Cantalapiedra et al. (2021)) was then  
163 performed to assign KEGG Orthology (KO) and identify specific functional annotation for the catalog of non-redundant  
164 genes. The marker genes, *nifDK* (K02586, K02591 nitrogenase molybdenum-iron protein alpha/beta chain) and *nifH*  
165 (K02588, nitrogenase iron protein), were used for the evaluation of microbial potential of  $\text{N}_2$  fixation. *RbcL* (K01601,  
166 ribulose-bisphosphate carboxylase large chain) and *psbA* (K02703, photosystem II P680 reaction center D1 protein) were  
167 selected to evaluate the microbial potential of carbon fixation and photosynthesis, respectively. The molecular datasets  
168 have been deposited with the accession number: Bioproject PRJNA1133027.

### 169 3 Results and discussion

#### 170 3.1 Hydrographic conditions in Qeqertarsuaq (Disco Bay) and Sullorsuaq (Vaigat) Strait

172 Disko Bay (Qeqertarsuaq) is located along the west coast of Greenland (Kalaallit Nunaat) at approximately 69 °N (Figure  
173 1), and is strongly influenced by the West Greenland Current (WGC) which is associated with the broader Baffin Bay Polar  
174 Waters (BBPW) (Mortensen et al., 2022; Hansen et al., 2012). The WGC does not only significantly shape the hydrographic  
175 conditions within the bay but also plays an important role in the larger context of Greenland Ice Sheet melting (Mortensen  
176 et al. (2022)). Central to the hydrographic system of the Qeqertarsuaq area is the Jakobshavn Isbræ, which is the most  
177 productive glacier in the northern hemisphere and believed to drain about 7 % of the Greenland Ice Sheet and thus  
178 contributes substantially to the water influx into the Qeqertarsuaq (Holland et al. (2008)). A predicted increased inflow of  
179 warm subsurface water, originating from North Atlantic waters, has been suggested to further affect the melting of the  
180 Jakobshavn Isbræ and thus adds another layer of complexity to this dynamic system (Holland et al., 2008; Hansen et al.,  
181 2012).

182 The hydrographic conditions in Qeqertarsuaq have a significant influence on biological processes, nutrient availability, and the



184

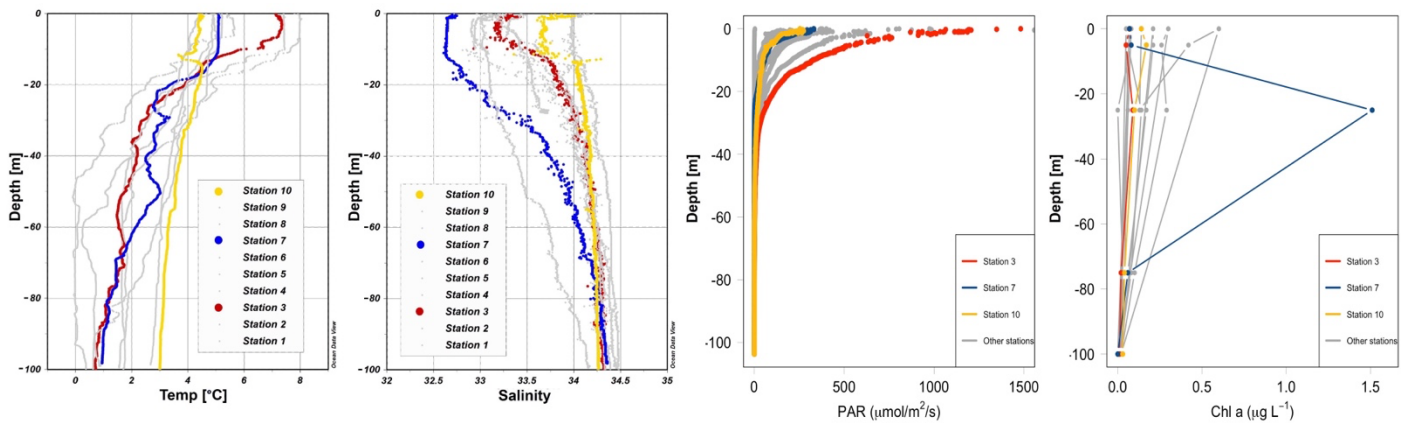
185 **Figure 1.** Map of Greenland (Kalaallit Nunaat) with indication of study area (red box), on the left. Interpolated distribution of Sea  
186 Surface Salinity (SSS) values with corresponding isosurface lines and indication of 10 sampled stations (normal stations in black,  
187 incubation stations in blue), black arrows indicate the West Greenland Current (WGC) and the black box indicate the location of the  
188 Jakobshavn Isbræ, in the middle. Scatterplot of the potential temperature and salinity for all station data. The plot is used for the  
189 identification of the main water masses within the study area. Isopycnals ( $\text{kg m}^{-3}$ ) are depicted in grey lines, on the right. Figures were  
190 created in Ocean Data View (ODV) (Schlitzer (2022)).

191 broader marine ecosystem (Munk et al., 2015; Hendry et al., 2019; Schiøtt, 2023).

192 During our survey, we found very heterogenous hydrographic conditions at the different stations across Qeqertarsuaq (Fig.  
193 1 & Fig. 2). The three selected stations for  $\text{N}_2$  fixation analysis (stations 3, 7, and 10) were strategically chosen to capture the

195 spatial

196 variability of the area. Surface salinity and temperature measurements at these stations indicate the influence of freshwater  
197 input. The surface temperature exhibit a range of 4.5 to 8 °C, while surface salinity varies between 31 and 34, as illustrated  
198 in Fig. 1. The profiles sampled during our survey extend to a maximum depth of 100 m. Comparison of temperature/salinity  
199 (T/S) plots with recent studies suggests the presence of previously described water masses, including Warm Fjord Water  
200 (WFjW) and Cold Fjord Water (CFjW) with an overlaying surface glacial meltwater runoff. Those water masses are defined  
201 with a density range of  $27.20 \leq \sigma_0 \leq 27.31$  but different temperature profiles. Thus water masses can be differentiated by  
202 their temperature within the same density range (Gladish et al. (2015)). Other water masses like upper subpolar mode water  
203 (uSPMW), deep subpolar mode water (dSPMW) and Baffin Bay polar Water (BBPW) which has been identified in the  
204 Disko Bay (Qeqertarsuaq) before, cannot be identified from this data and may be present in deeper layers (Mortensen et  
205 al., 2022; Sherwood et al., 2021; Myers and Ribergaard, 2013; Rysgaard et al., 2020). The temperature and salinity profiles  
206 across the 10



207  
208  
209  
210 **Figure 2.** Profiles of temperature (°C), salinity, photosynthetically active radiation (PAR) ( $\mu\text{mol}/\text{m}^2/\text{s}$ ) and Chl  $a$  ( $\text{mg m}^{-3}$ ) across stations  
211 1 to 10 with depth (m). Stations 3, 7, and 10 are highlighted in red, blue, and yellow, respectively, to emphasize incubation stations.  
212 Figures were created in Ocean Data View and R-Studio (Schlitzer (2022)).

213 stations in the study area show distinct stratification and variability, which is represented through the three incubation  
214 stations (highlighted stations 3, 7, and 10 in Fig. 2). They display varying degrees of stratification and mixing, with notable  
215 differences in the salinity and temperature profiles. Station 3 and station 7 exhibit clear stratification in both temperature  
216 and salinity marked by the presence of thermoclines and haloclines. These features suggest significant freshwater input  
217 influenced by local weather conditions and climate dynamics, like surface heat absorption. In contrast, Station 10 exhibits a  
218 narrower range of temperature and salinity values throughout the water column compared to Stations 3 and 7, indicating  
219 more well-mixed conditions. This uniformity is likely influenced by the regional circulation pattern and partial upwelling  
220 (Hansen et al., 2012; Krawczyk et al., 2022). The distinct characteristics observed at station 10, as illustrated in the surface  
221

222 plot (Fig. 1), show an elevated salinity and colder temperatures compared  
223 to the other stations. This feature suggests upwelling of deeper waters along the shallower shelf, likely facilitated by the  
224 local seafloor topography. Specifically, the seafloor shallowing off the coast of Station 10 may act as a barrier, disrupting  
225 typical circulation and forcing deeper, saltier, and colder waters to the surface. This pattern aligns with previous studies that  
226 describe similar mechanisms in the region (Krawczyk et al. (2022)). Their description of the bathymetry in Qeqertarsuaq,  
227 featuring depths ranging from ca. 50 to 900 m, suggests its impact on turbulent circulation patterns, leading to the mixing  
228 of different water masses. Evident variability in oceanographic conditions that can be observed throughout the study area  
229 occurs particularly along characteristic topographical features like steep slopes, canyons, and shallower areas. The summer  
230 melting of sea ice and glaciers introduces freshwater influxes that create distinct vertical and horizontal gradients in salinity  
231 and temperature in the Qeqertarsuaq area Hansen et al. (2012). Additionally, the accelerated melting of the Jakobshavn  
232 Isbraæ, influenced by the warmer inflow from the West Greenland Intermediate Current (WGIC), further alters the  
233 hydrographic conditions. Recent observations indicate significant warming and shoaling of the WGIC, potentially enabling  
234 it to overcome the sill separating the Illulissat Fjord from the Qeqertarsuaq area (Hansen et al., 2012; Holland et al., 2008;  
235 Myers and Rønne, 2013). This shift intensifies glacier melting, driving substantial changes in the local ecological  
236 dynamics (Ardyna et al., 2014; Arrigo et al., 2008; Bhatia et al., 2013).

### 237 **3.2 Elevated N<sub>2</sub> fixation rates might play a role in nutrient dynamics and bloom development**

238 We quantified N<sub>2</sub> fixation rates within the waters of Qeqertarsuaq, spanning from the surface to a depth of 50 m (Table 1).  
239 The rates ranged from 0.16 to 2.71 nmol N L<sup>-1</sup> d<sup>-1</sup> with all rates surpassing the detection limit. Our findings represent  
240 rates at the upper range of those observed in the Arctic Ocean. Previous measurements in the region have been limited,  
241 with only one study in Baffin Bay by Blais et al. (2012), reporting rates of 0.02 nmol N L<sup>-1</sup> d<sup>-1</sup>, which are 1-2 orders of  
242 magnitude lower than our observations. Moreover, Sipler et al. (2017), reported rates in the coastal Chukchi Sea, with  
243 average values of 7.7 nmol N L<sup>-1</sup> d<sup>-1</sup>. These values currently represent some of the highest rates measured in Arctic shelf  
244 environments. Compared to these, our highest measured rate (2.71 nmol N L<sup>-1</sup> d<sup>-1</sup>) is slower, but still substantial,  
245 particularly considering the more Atlantic-influenced location of our study site. Sipler et al. (2017) also noted that a  
246 significant fraction of diazotrophs were <3 µm in size, suggesting that small unicellular diazotrophs play a dominant role  
247 in Arctic nitrogen fixation. Altogether, our data contribute to the growing evidence that N<sub>2</sub> fixation is a widespread and  
248 potentially significant nitrogen source across various Arctic regions. Simultaneous primary production rate measurements  
249 ranged from 0.07 to 3.79 µmol N L<sup>-1</sup> d<sup>-1</sup>, with the highest rates observed at station 7 and generally higher values in the surface  
250 layers. Employing Redfield stoichiometry, the measured N<sub>2</sub> fixation rates accounted for 0.47 to 2.6 % (averaging 1.57 %) of  
251 primary production at our stations. The modest contribution to primary production suggests that N<sub>2</sub> fixation does not exert  
252 a substantial influence on the productivity of these waters during the time of the sampling. Rather, our N<sub>2</sub> fixation rates  
253 suggest primary production to depend mostly on additional nitrogen sources including regenerated, meltwater or land-based  
254 sources.

256 While the N:P ratio is commonly used to assess nutrient limitations relative to Redfield stoichiometry, most DIN and DIP  
 257 measurements in our study were below detection limit (BDL), preventing a reliable calculation for this ratio. As such, we  
 258 refrain from drawing conclusions based on N:P stoichiometry. Nevertheless, previous studies by Jensen et al. (1999) and  
 259 Tremblay and Gagnon (2009), have identified nitrogen limitation in this region. Such biogeochemical conditions, when present,  
 260 would be expected to generate a niche for N<sub>2</sub> fixing organisms (Sohm et al. (2011)).  
 261 While N<sub>2</sub> fixation did not chiefly sustain primary production during our sampling campaign, we hypothesize that N<sub>2</sub> fixation  
 262 has the potential to play a role in bloom dynamics. As nitrogen availability decreases  
 263 during a bloom, it may provide a niche for N<sub>2</sub> fixation, potentially extending the productive period of the bloom (Reeder et  
 264 al. (2021)). Satellite data indicates that a fall bloom began in early August, following the annual spring bloom, as described  
 265 by Ardyna et al. (2014). This double bloom situation may be driven by increased melting and the subsequent input of  
 266 bioavailable nutrients and iron (Fe) from meltwater runoff (Arrigo et al., 2017; Hopwood et al., 2016; Bhatia et al., 2013).  
 267 The meltwater from the Greenland Ice Sheet is a significant source of Fe (Bhatia et al., 2013; Hawkings et al., 2015, 2014),  
 268 which is a limiting factor especially for diazotrophs (Sohm et al. (2011)). Consequently, it is possible that nutrients and Fe  
 269 from the Isbræ glacier introduced into the Qeqertarsuaq are promoting a bloom and further provide a niche for diazotrophs  
 270 to thrive (Arrigo et al. (2017)).

271  
 272  
 273  
 274  
 275  
 276

**Table 1.** N<sub>2</sub> fixation (nmol N L<sup>-1</sup> d<sup>-1</sup>), standard deviation (SD), primary productivity (PP;  $\mu\text{mol C L}^{-1} \text{d}^{-1}$ ), SD, percentage of estimated new primary productivity (% New PP) sustained by N<sub>2</sub> fixation, dissolved inorganic nitrogen compounds (NO<sub>x</sub>), phosphorus (PO<sub>4</sub>) at stations 3, 7, and 10. BDL = Below detection limit.

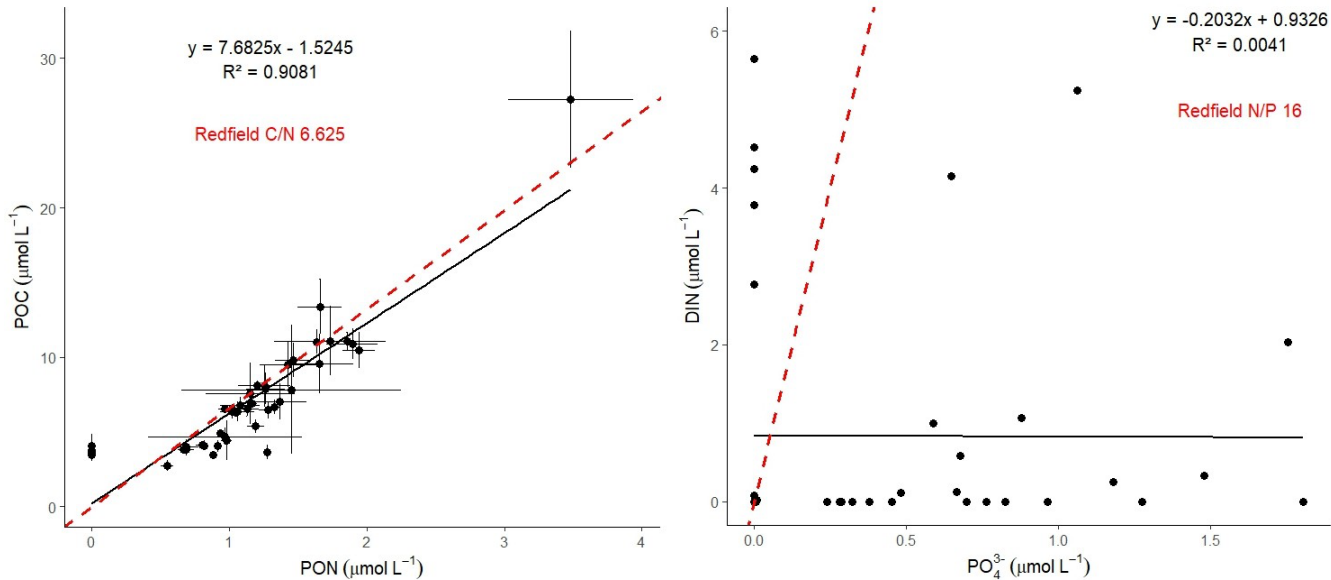
Station (no.)	Depth (m)	N <sub>2</sub> fixation (nmol N L <sup>-1</sup> d <sup>-1</sup> )	SD ( $\pm$ )	Primary Productivity ( $\mu\text{mol C L}^{-1} \text{d}^{-1}$ )	SD ( $\pm$ )	% New PP (%)	NO <sub>x</sub> ( $\mu\text{mol L}^{-1} \text{d}^{-1}$ )	PO <sub>4</sub> ( $\mu\text{mol L}^{-1} \text{d}^{-1}$ )
3	0	1.20	0.21	0.466	0.08	1.71	BDL	BDL
3	25	1.88	0.11	0.588	0.04	2.11	BDL	0.70
3	50	0.29	0.01	0.209	0.00	0.91	0.33	1.48
7	0	2.49	0.44	0.63	0.20	2.60	BDL	BDL
7	25	2.71	0.22	3.79	2.45	0.47	BDL	0.45
7	50	0.53	0.24	0.33	0.36	1.08	BDL	0.97
10	0	1.48	0.12	0.74	0.15	1.33	BDL	BDL
10	25	0.31	0.01	0.29	0.07	0.73	BDL	BDL
10	50	0.16	0	0.07	0.07	1.40	BDL	BDL

277  
 278 A near-Redfield stoichiometry in POC:PON suggests that the particulate organic matter (POM) likely originates from an

ongoing phytoplankton bloom, as phytoplankton generally assimilate carbon and nitrogen in relatively consistent proportions during active growth (Redfield 1934). However this assumption is based on a global average, and POM stoichiometry can exhibit substantial latitudinal variation. Deviations may also arise during particle production and remineralization processes (Redfield 1934; Geider and La Roche 2002; Sterner and Elser 2017; Quigg et al., 2003). Recent studies have further shown that POM composition vary widely across plankton communities, influenced by factors such as growth rates, community composition, and physiological status (e.g. fast- vs- slow-growing organisms), with degradation often playing a secondary role (Tanioka et al., 2022). Additionally, terrestrial organic material—likely introduced via glacial outflow in the study area—may also contribute to the observed POM composition (Schneider et al., 2003). Latitudinal variability in organic matter stoichiometry has also been linked to differences in nutrient supply and phosphorus stress (Fagan et al., 2024; Tanioka et al., 2022). Consequently, the near-Redfield stoichiometry observed here cannot be clearly attributed to freshly produced organic material. Nevertheless, satellite-derived surface chlorophyll *a* concentrations and associated primary production support the interpretation that recently produced organic matter does contribute, at least in part, to the sinking POM captured in our samples. Since inorganic nitrogen species (e.g., NOx) were below detection limits, direct calculation or interpretation of the N:P ratio in the dissolved nutrient pool was not possible and has been avoided. The absence of available nitrogen may nonetheless reflect nitrogen depletion, potentially creating ecological niches for diazotrophs and nitrogen-fixing organisms. Such conditions may promote shifts in microbial community structure, as observed by Laso-Perez et al. (2024). Laso Perez et al. (2024) documented changes in microbial community composition during an Arctic bloom, focusing on nitrogen cycling. They observed a shift from chemolithotrophic to heterotrophic organisms throughout the summer bloom and noted increased activity to compete for various nitrogen sources. However, no *nifH* gene copies, indicative of nitrogen-fixing organisms, were found in their dataset based on metagenome-assembled genomes (MAGs). This is not unexpected due to the classically low abundance of diazotrophs in marine microbial communities which has often been described (Turk-Kubo et al., 2015; Farnelid et al., 2019). Given the high productivity and metabolic activity observed in Qeqertarsuaq during a similar bloom period, the detected diazotrophs (Section 3.3) may play a more significant role than previously thought. Across the 10 stations there is considerable variability in POC and PON concentrations (Fig. 3). PON concentrations range from 0.0  $\mu\text{mol N L}^{-1}$  to 3.48  $\mu\text{mol N L}^{-1}$  (n=124), while POC concentrations range from 2.7  $\mu\text{mol C L}^{-1}$  to 27.2  $\mu\text{mol C L}^{-1}$  (n=144). The highest concentrations for both PON and POC were observed at station 7 at a depth of 25 m and coincide with the highest reported N<sub>2</sub> fixation rate (Figure Appendix A2 & A3). Generally, POC and PON concentrations decrease with depth, peaking at the deep chl *a* maximum (DCM), identified between 15 to 30 m across all stations. The DCM was identified based on measured chl *a* concentrations and previous descriptions in the region (Fox and Walker, 2022; Jensen et al., 1999). The variability in chl *a* concentrations indicates differences in phytoplankton abundance among the stations, with concentrations ranging between 0 to 0.42 mg m<sup>-3</sup>. Excluding station 7, which exhibited the highest chl *a* concentration at the DCM (1.51 mg m<sup>-3</sup>). While Tang et al. (2019) found that N<sub>2</sub> fixation measurements strongly correlated to satellite estimates of chl *a* concentrations, our results did not show a statistically significant correlation between nitrogen fixation rates and chl *a* concentrations overall

313 (Figures A2 & A3). However, as noted, Station 7 at 25 m represents a unique case. The elevated concentration of chl *a* at  
 314 this station likely resulted from a local phytoplankton bloom induced by meltwater outflow from the Isbræ glacier and sea  
 315 ice melting, which may help explain the observed nitrogen fixation rates (Arrigo et al., 2017; Wang et al., 2014). This  
 316 study's findings are in agreement with prior reports of analogous blooms occurring in the region (Fox and Walker, 2022;  
 317 Jensen et al., 1999).

318



319

320

321

322

### 323 3.3 Potential Contribution of UCYN-A to Nitrogen Fixation During a Diatom Bloom: Insights and Uncertainties

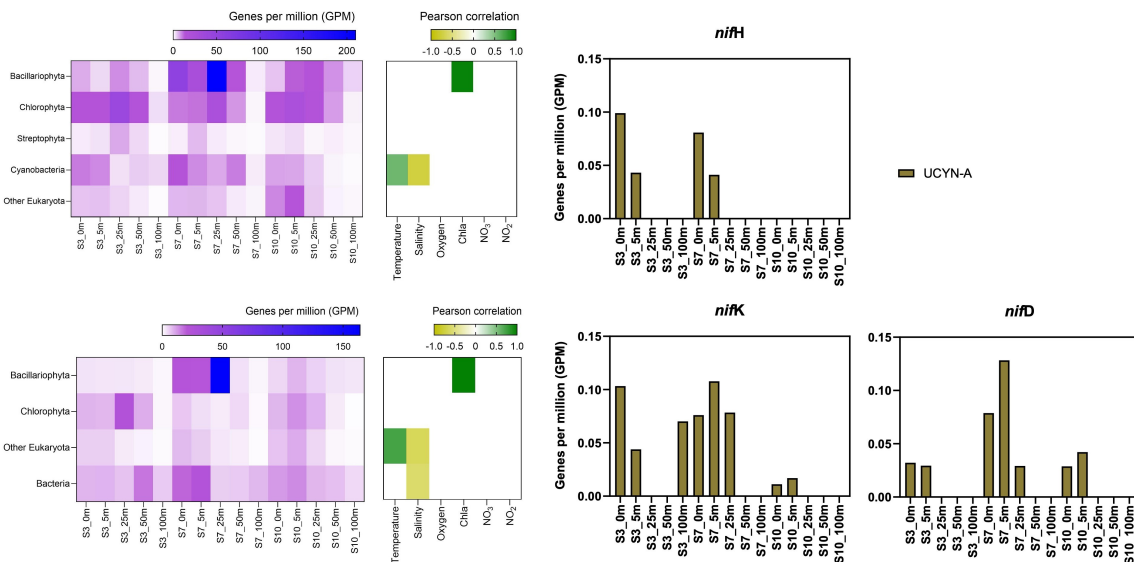
324 In our metagenomic analysis, we filtered the *nifH*, *nifD*, *nifK* genes, which code for the nitrogenase enzyme responsible  
 325 for catalyzing  $\text{N}_2$  fixation. We could identify sequences related to UCYN-A, which dominated the sequence pool of  
 326 diazotrophs, particularly in the upper water masses (0 to 5 m) (Fig. 4). UCYN-A, a unicellular cyanobacterial symbiont, has  
 327 a cosmopolitan distribution and is thought to substantially contribute to global  $\text{N}_2$  fixation, as documented by (Martínez-  
 328 Pérez et al., 2016; Tang et al., 2019). This conclusion is based on our metagenomic analysis, in which we set a sequence  
 329 identity threshold of 95% for both *nif* and photosystem genes. Notably, we only recovered sequences related to UCYN-A  
 330 within our *nif* sequence pool, suggesting its predominance among detected diazotrophs. However, metagenomic  
 331 approaches may underestimate overall diazotroph diversity, and we cannot fully exclude the presence of other, less  
 332 abundant diazotrophs that may have been missed using this method. While UCYN-A was primarily detected in surface  
 333 waters, we also observed relatively high *nifK* values at S3\_100m, an unusual finding given that UCYN-A is typically  
 334

335 constrained to the euphotic zone. Previous studies have predominantly reported UCYN-A in surface waters; for instance  
336 Harding et al. (2018) and Shiozaki et al. (2017) detected UCYN-A exclusively in the upper layers of the Arctic Ocean.  
337 Additionally, Shiozaki et al. (2020) found UCYN-A2 at depths extending to the 0.1% light level but not below 66 m in the  
338 Chukchi Sea. The detection of UCYN-A at 100 m in our study suggests that alternative mechanisms, such as particle  
339 association, vertical transport, or local environmental conditions, may facilitate its presence at depth. This warrants further  
340 investigation into the potential processes enabling its occurrence below the euphotic zone.

341 Due to the lack of genes such as those encoding Photosystem II and Rubisco, UCYN-A plays a significant role within the  
342 host cell and participates in fundamental cellular processes. Consequently it has evolved to become a closely integrated  
343 component of the host cell. Very recent findings demonstrate that UCYN-A imports proteins encoded by the host genome  
344 and has been described as an early form of N<sub>2</sub> fixing organelle termed a "Nitroplast" (Coale et al. (2024)).

345 Previous investigations document that they are critical for primary production, supplying up to 85% of the fixed nitrogen to  
346 their haptophyte host (Martínez-Pérez et al. (2016)). In addition to its high contribution to primary production, studies have  
347 shown that UCYN-A in high latitude waters fix similar amounts of N<sub>2</sub> per cell as in the tropical Atlantic Ocean, even in  
348 nitrogen- replete waters (Harding et al., 2018; Shiozaki et al., 2020; Martínez-Pérez et al., 2016; Krupke et al., 2015; Mills  
349 et al., 2020). However, estimating their contribution to N<sub>2</sub> fixation in our study is challenging, particularly since we detected  
350 cyanobacteria only at the surface but observe significant N<sub>2</sub> fixation rates below 5 m. The diazotrophic community is often  
351 underrepresented in metagenomic datasets due to the low abundance of nitrogenase gene copies, implying our data does  
352 not present a complete picture. We suspect a more diverse diazotrophic community exists, with UCYN-A being a significant  
353 contributor to N<sub>2</sub> fixation in Arctic waters. However, the exact proportion of its contribution requires further investigation.  
354 The contribution of N<sub>2</sub> fixation to carbon fixation (as percent of PP) is relatively low, at the time of our study. We identified  
355 genes such as *rbcL*, which encodes Rubisco, a key enzyme in the carbon fixation pathway and *psbA*, a gene encoding  
356 Photosystem II, involved in light-driven electron transfer in photosynthesis, in our metagenomic dataset. The gene *rbcL* (for  
357 the carbon fixation pathway) and the gene *psbA* (for primary producers) were used to track the community of photosynthetic  
358 primary producers in our metagenomic dataset. At station 7, elevated carbon fixation rates are correlated with high diatom  
359 (*Bacillariophyta*) abundance and increased chl *a* concentration (Fig. 4), suggesting the onset of a bloom, which is also  
360 observable via satellite images (Appendix A1). We hypothesize that meltwater, carrying elevated nutrient and trace metal  
361 concentrations, was rapidly transported away from the glacier through the Vaigat Strait by strong winds, leading to increased  
362 productivity, as previously described by Fox and Walker (2022) & Jensen et al. (1999). The elevated diatom abundance and  
363 primary production rates at station 7 coincide with the highest N<sub>2</sub> fixation rates, which could possibly point toward a possible  
364 diatom-diazotroph symbiosis (Foster et al., 2022, 2011; Schvarcz et al., 2022). However, we did not detect a clear  
365 diazotrophic signal directly associated with the diatoms in our metagenomic dataset, which might be due to generally  
366 underrepresentation of diazotrophs in metagenomes due to low abundance or low sequencing coverage. To investigate  
367 this further, we examined the taxonomic composition of *Bacillariophyta* at higher resolution. Among the various  
368 abundant diatom genera, *Rhizosolenia* and *Chaetoceros* have been identified as symbiosis with diazotrophs (Grosse,

369 *et al.*, 2010; Foster, *et al.*, 2010), representing less than 6% or 15% of *Bacillariophyta*, based on *rbcL* or *psbA*,  
 370 respectively (Figure Appendix A4). Although we underestimate diazotrophs to an extent, the presence of certain  
 371 diatom-diazotroph symbiosis could help explain the high nitrogen fixation rates in the diatom bloom to a certain  
 372 degree. Compilation of *nif* sequences identified from this study as well as homologous from their NCBI top hit were  
 373 added in Table S1. However, we cannot tell if the diazotrophs belong to UCYN-A1 or UCYN-A2, or UCYN-A3.  
 374 Based on the Pierella Karlusich *et al.* (2021), they generated clonal *nifH* sequences from Tara Oceans, which the  
 375 length of *nifH* sequences is much shorter than the two *nifH* sequences we generated in our study. Also, the available  
 376 UCYN-A2 or UCYN-A3 *nifH* sequences from NCBI were shorter than the two *nifH* sequences we generated.  
 377 Therefore, it would be not accurate to assign the *nifH* sequences to either group under UCYN-A. Furthermore, not  
 378 much information is available regarding the different groups of UCYN-A using marker genes of *nifD* and *nifK*.  
 379



380  
381

382

383 **Figure 4.** Upper left image: *psbA* with correlation plot. Lower left image: *rbcL* with correlation plot. Right image: *nifH*, *nifD*, *nifK*  
 384 genes per million reads in the metagenomic datasets. All figures display molecular data from metagenomic dataset for all sampled depth  
 385 of station 3,7,10

386

387

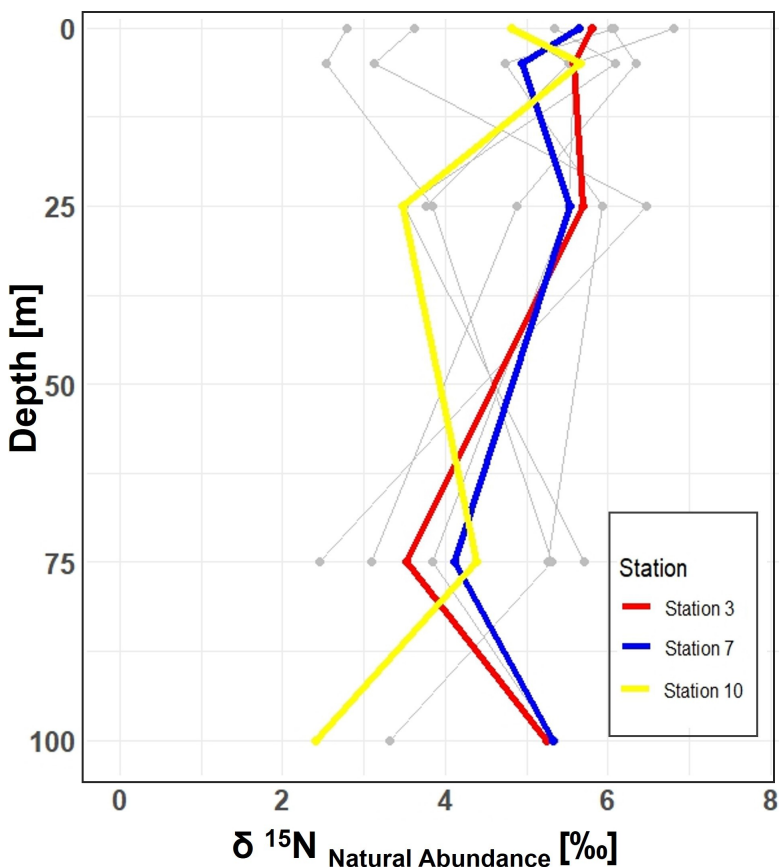
388 There is evidence that UCYN-A have a higher Fe demand, with input through meltwater or river runoff potentially being  
 389 advantageous to those organisms (Shiozaki *et al.*, 2017, 2018; Cheung *et al.*, 2022). Consequently, UCYN-A might play a  
 390 more critical role in the future with increased Fe-rich meltwater runoff. UCYN-A can potentially fuel primary productivity  
 391 by supplying nitrogen, especially with increased melting, nutrient inputs, and more light availability due to rising  
 392 temperatures as- sociated with climate change. This predicted enhancement of primary productivity may contribute to the  
 biological drawdown of CO<sub>2</sub>, acting as a negative feedback mechanism. These projections are based on studies forecasting

393 increased temperatures, melting, and resulting biogeochemical changes leading to higher primary productivity. However  
394 large uncertainties make predictions very difficult and should be handled with care. Thus we can only hypothesize that  
395 UCYN-A might be coupled to these dynamics by providing essential nitrogen.

396 **3.4  $\delta^{15}\text{N}$  Signatures in particulate organic nitrogen**

397 Stable isotopic composition, expressed using the  $\delta^{15}\text{N}$  notation, serve as indicators for understanding nitrogen dynamics  
398 because different biogeochemical processes fractionate nitrogen isotopes in distinct ways (Montoya (2008)). However, it  
400 is important to keep in mind that the final isotopic signal is a combination of all processes and an accurate distinction  
401 between processes cannot be made.  $\text{N}_2$  fixation tends to enrich nitrogenous compounds with lighter isotopes, producing  
402 OM with isotopic values ranging approximately from -2 to +2 ‰ (Dähnke and Thamdrup (2013)). Upon complete  
403 remineralization and oxidation, organic matter contributes to a reduction in the average  $\delta$ -values in the open ocean  
404 (e.g. Montoya et al. (2002);

405 Emeis et al. (2010)). Whereas processes like denitrification and anammox preferentially remove lighter isotopes, leading  
406 to enrichment in heavier isotopes and delta values up to -25 ‰.



408

409

410 **Figure 5.** Vertical profiles of  $\delta^{15}\text{N}$  natural abundance signatures in PON across 10 stations in the study area. Incubation stations 3, 7, and  
411 10 are highlighted in red, blue, and yellow, respectively. The figure shows variations in  $\delta^{15}\text{N}$  signatures with depth at each station,  
412 providing insight into nitrogen cycling in the study area.

413

414 In our study, the  $\delta^{15}\text{N}$  values of PON from all 10 stations, range between 2.45 ‰ and 8.30 ‰ within the 0 to 100 m depth  
415 range. While  $\text{N}_2$  fixation typically produces OM ranging from -2 ‰ to 0.5 ‰, this signal can be masked by processes such as  
416 remineralization, mixing with nitrate from deeper waters or other biological transformations (Emeis et al. (2010); Sigman  
417 et al. (2009)). The composition of OM in the surface ocean is influenced by the nitrogen substrate and the fractionation  
418 factor during assimilation. When nitrate is depleted in the surface ocean, the isotopic signature of OM produced during  
419 photosynthesis will mirror that of the nitrogen source. Nitrate, the primary form of dissolved nitrogen in the open ocean,  
420 typically exhibits an average stable isotope value of around

421

422 5 ‰. No fractionation occurs during photosynthesis because the nitrogen source is entirely taken up in the surface waters  
423 (Sigman et al. (2009)). This matches conditions observed in Qeqertarsuaq, suggesting that subsurface nitrate is a dominant  
424 nitrogen source. (Fox and Walker (2022)).

425

426 In the eastern Baffin Bay waters, Atlantic water masses serve as an important source of nitrate to surface waters, with  $\delta^{15}\text{N}$   
427 values around 5 ‰ (Sherwood et al. (2021)). This is consistent with our observed PON values and supports the view that  
428 primary productivity in the region is largely fueled by nitrate input from deeper Atlantic waters, particularly during early  
429 bloom stages (Fox and Walker, 2022; Knies, 2022). The mechanisms through which subsurface nitrate reaches the euphotic  
430 layer are not well understood. However, potential pathways include vertical migration of phytoplankton and physical  
431 mixing. Subsequently, nitrogen undergoes rapid recycling and remineralization processes to meet the system's nitrogen  
432 demands (Jensen et al. (1999)). Taken together, the  $\delta^{15}\text{N}$  signatures observed in this study are best interpreted as indicative  
433 of a system influenced by multiple nitrogen sources and biogeochemical processes, where nitrate input and remineralization  
434 appear to dominate.

435

436

437

438

439

440

441

442

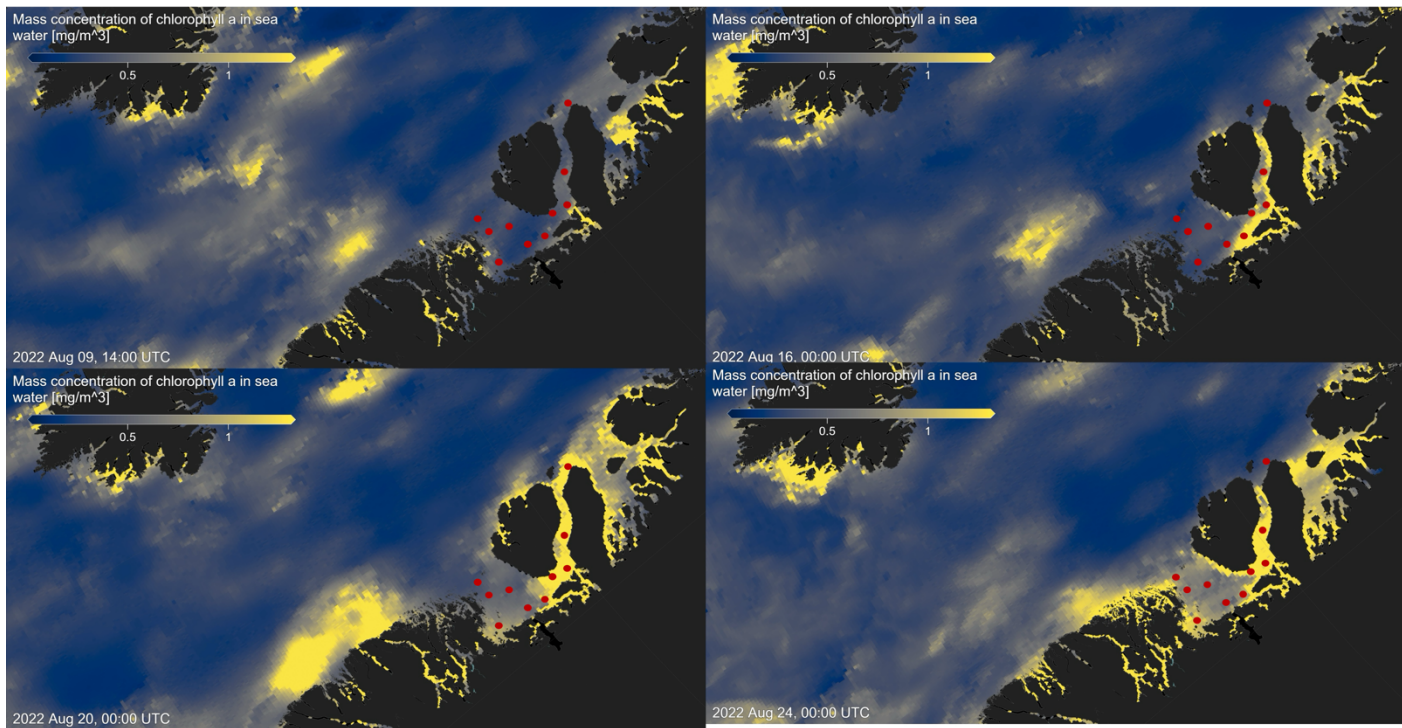
#### 4 Conclusion

Our study highlights the occurrence of elevated rates of  $\text{N}_2$  fixation in Arctic coastal waters, particularly prominent at station 7, where they coincide with high chl *a* values, indicative of heightened productivity. Satellite observations tracing the origin of a bloom near the Isbræ Glacier, subsequently moving through the Vaigat strait, suggest a recurring phenomenon likely triggered by increased nutrient-rich meltwater originating from the glacier. This aligns with previous reports by Jensen et al. (1999) & Fox and Walker (2022), underlining the significance of such events in driving primary productivity in the region. The contribution of  $\text{N}_2$  fixation to primary production was low (average 1.57 %) across the stations. Since the demand was high relative to the new nitrogen provided by  $\text{N}_2$  fixation, the observed primary production must be sustained by the already

443 present or adequate amount of subsurface supply of  $\text{NO}_x$  nutrients in the seawater. This is also visible in the isotopic signature  
444 of the POM (Fox and Walker, 2022; Sherwood et al., 2021). However, the detected  $\text{N}_2$  fixation rates are likely linked to the  
445 development of the fresh secondary summer bloom, which could be sustained by high nutrient and Fe availability from  
446 melting, potentially leading the system into a nutrient-limited state. The ongoing high demand for nitrogen compounds may  
447 suggest an onset to further sustain the bloom, but it remains speculative whether Fe availability definitively contributes to  
448 this process. The occurrence of such double blooms has increased by 10 % in the Qeqertarsuaq and even 33 % in the Baffin  
449 Bay, with further projected increases moving north from Greenland (Kalaallit Nunaat) waters (Ardyna et al. (2014)). Thus,  
450 nutrient demands are likely to increase, and the role of  $\text{N}_2$  fixation can become more significant. The diazotrophic  
451 community in this study is dominated by UCYN-A in surface waters and may be linked to diatom abundance in deeper  
452 layers. This co-occurrence of diatoms and  $\text{N}_2$  fixers in the same location is probably due to the co-limitation of similar  
453 nutrients, rather than a symbiotic relationship. Thus, this highlights the significant presence of diazotrophs despite their  
454 limited representation in datasets. It also highlights the potential for further discoveries, as existing datasets likely  
455 underestimate the full extent of the diazotrophic community (Laso Perez et al., 2024;  
456 Shao et al., 2023; Shiozaki et al., 2017, 2023). The reported  $\text{N}_2$  fixation rates in the Vaigat strait within the Arctic Ocean  
457 are notably higher than those observed in many other oceanic regions, emphasizing that  $\text{N}_2$  fixation is an active and  
458 significant process in these high-latitude waters. When compared to measured rates across various ocean systems using the  
459  $^{15}\text{N}$  approach, the significance of these findings becomes clear. For instance,  $\text{N}_2$  fixation rates are sometimes below the  
460 detection limit and often relatively low ranging from 0.8 to 4.4 nmol  $\text{N L}^{-1} \text{d}^{-1}$  (Löscher et al., 2020, 2016; Turk et al., 2011).  
461 In contrast, higher rates reach up to 20 nmol  $\text{N L}^{-1} \text{d}^{-1}$  (Rees et al. (2009)) and sometime exceptional high rates range from  
462 38 to 610 nmol  $\text{N L}^{-1} \text{d}^{-1}$  (Bonnet et al. (2009)). The Arctic Ocean rates are thus significant in the global context,  
463 underscoring the region's role in the global nitrogen cycle and the importance of  $\text{N}_2$  fixation in supporting primary  
464 productivity in these waters.  
465 These findings highlight the urgent need to understand the interplay between seasonal variations, sea-ice dynamics, and  
466 hydro- graphic conditions in Qeqertarsuaq. As climate change accelerates the melting of the Greenland Ice Sheet at  
467 Jakobshavn Isbræ, shifts in hydrodynamic patterns and hydrographic conditions in Qeqertarsuaq are anticipated. The  
468 resulting influx of warmer waters could significantly reshape the bay's hydrography, making it crucial to comprehend the  
469 coupling of climate-driven changes and oceanic processes in this vital Arctic region. Our study provides key insights into  
470 these dynamics and underscores the importance of continued investigation to predict Qeqertarsuaq's future hydrographic  
471 state. By detailing the environmental and hydrographic changes, we contribute valuable knowledge to the broader context  
472 of  $\text{N}_2$  fixation in the Arctic Ocean. Given nitrogen's pivotal role in Arctic ecosystem productivity, it is essential to explore  
473 diazotrophs, quantify  $\text{N}_2$  fixation, and assess their impact on ecosystem services as climate change progresses.

474 **Appendix A**  
475

476



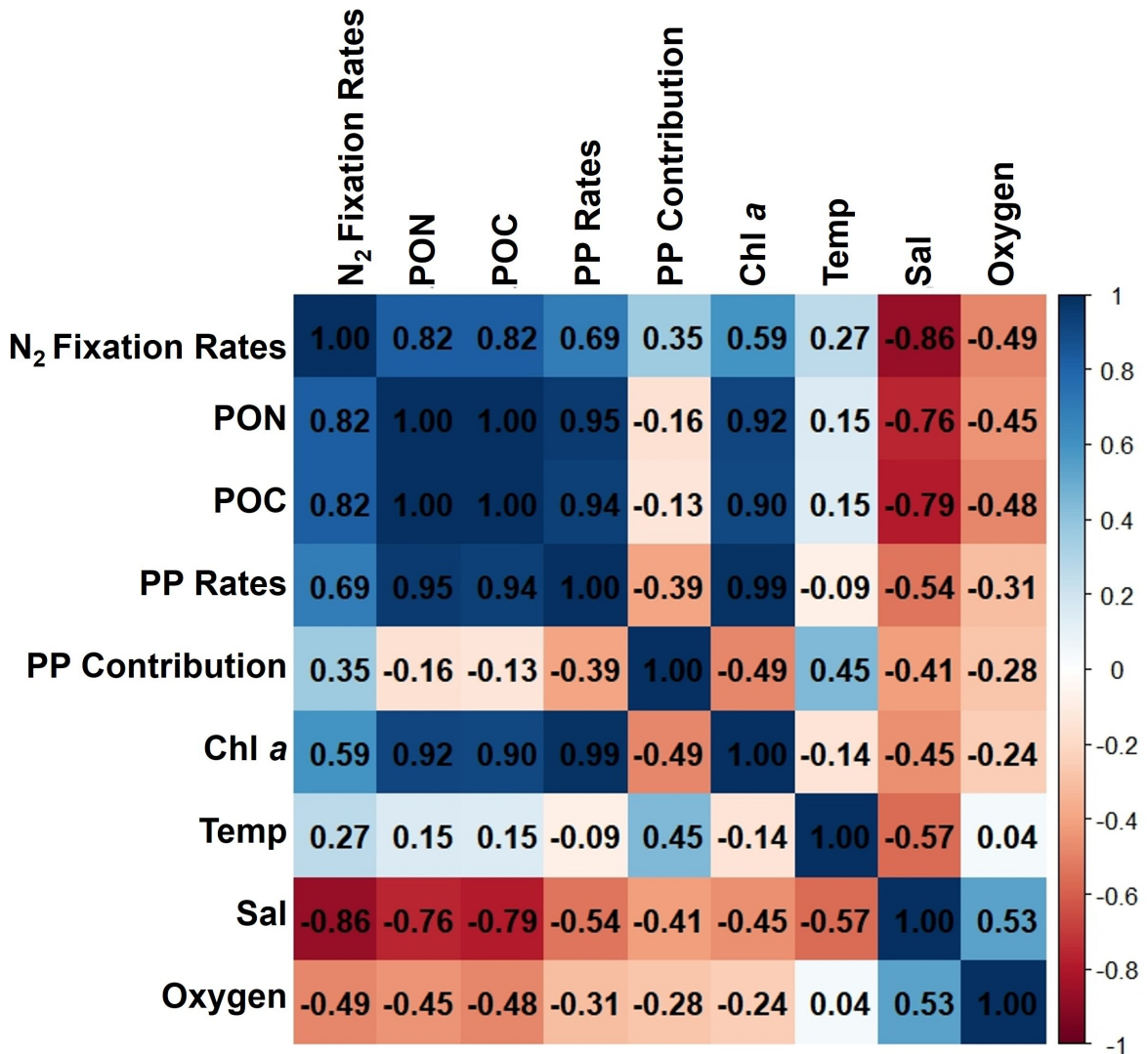
477

478

479

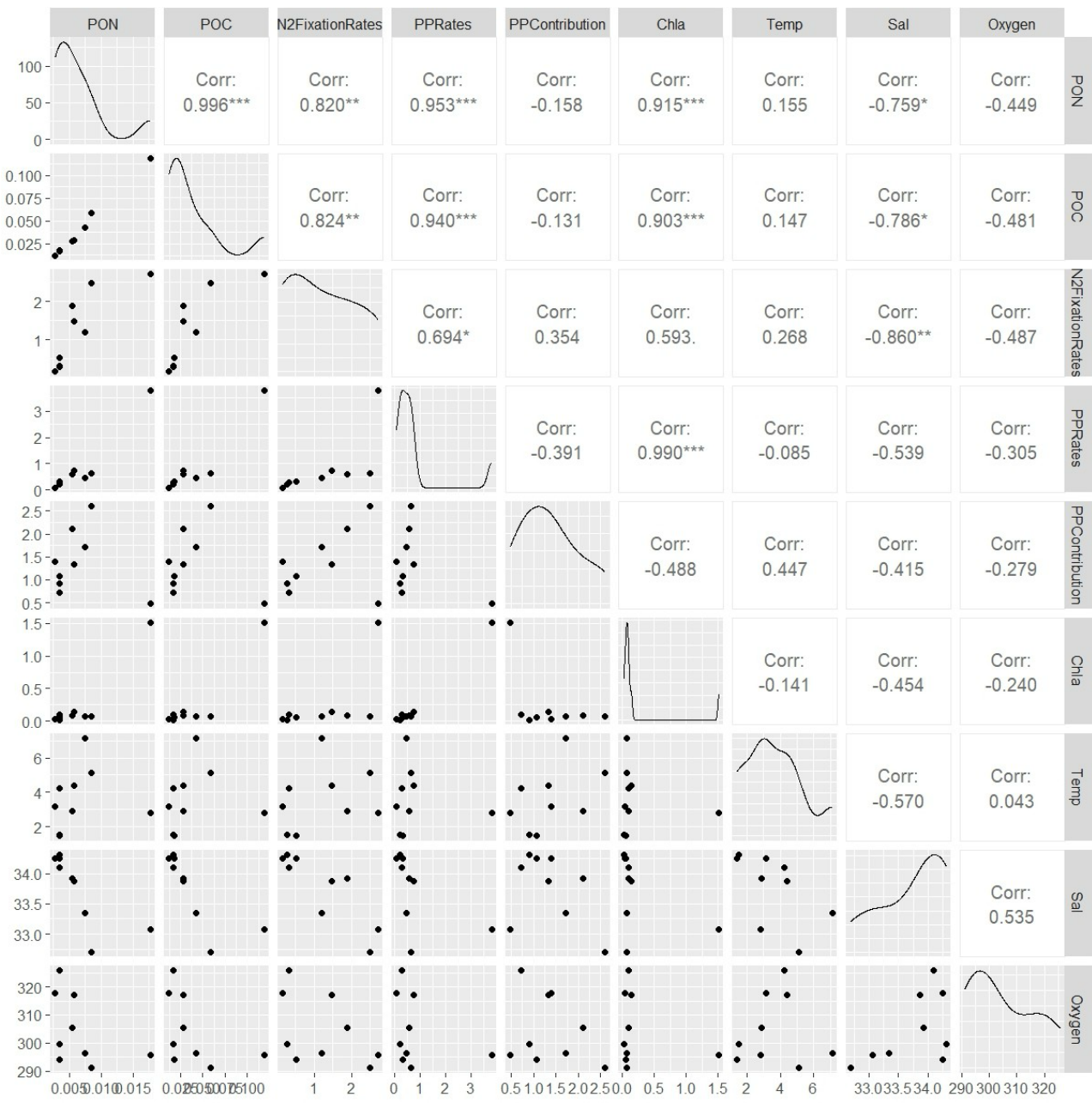
480

**Figure A1.** Chlorophyll  $a$  concentration  $\text{mg m}^{-3}$  at four time points before, during, and after sea water sampling in August 2022 (sampling stations indicated by red dots), obtained from MODIS-Aqua; <https://giovanni.gsfc.nasa.gov> (Aqua MODIS Global Mapped Chl  $a$  Data, version R2022.0, DOI:10.5067/AQUA/MODIS/L3M/CHL/2022), 4 km resolution, last access 03 June 2024

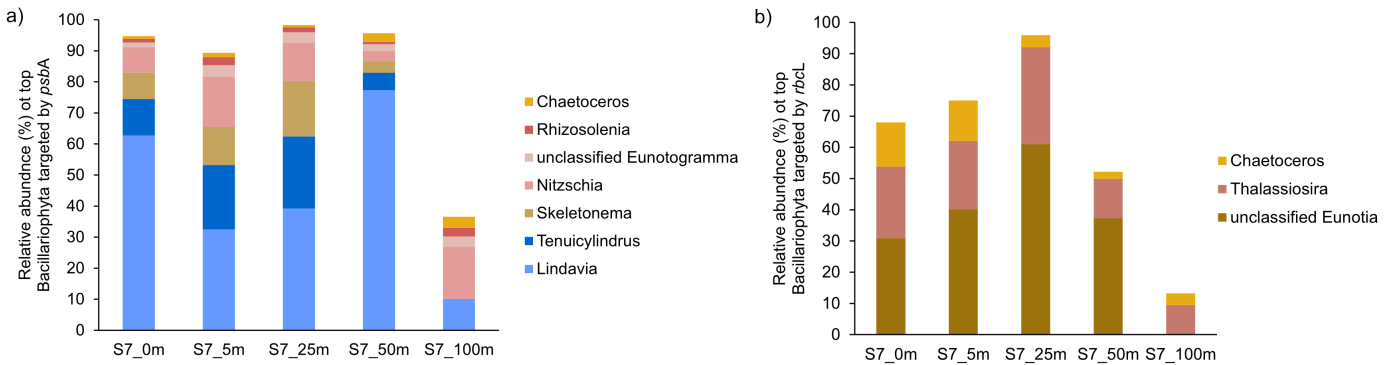


481  
482  
483  
484  
485  
486  
487

**Figure A2.** Correlation matrix of environmental and biological variables. The plot shows the correlation coefficients between the following parameters: N<sub>2</sub> fixation rates, PON, POC, PP rates, the contribution N<sub>2</sub> fixation to PP (PP contribution), Chl a, temperature (Temp), salinity (Sal), and Oxygen. The scale ranges from -1 to 1, where values close to 1 or -1 indicate strong positive or negative correlations, respectively, and values near 0 indicate weak or no correlation. The color intensity represents the strength and direction of the correlations, facilitating the identification of relationships among the variables



495  
496  
497



503 *Data availability.* The presented data collected during the cruise will be made accessible on PANGEA. The molecular datasets have  
504 been deposited with the accession number: Bioproject PRJNA1133027

505  
506  
507  
508 *Author contributions.* IS carried out fieldwork and laboratory work at the University of Southern Denmark, and wrote the majority of  
509 the manuscript. ELP, AM, and EL conducted fieldwork and laboratory work at the University of Southern Denmark. PX performed  
510 metagenomic analysis and created the corresponding graphs. CRL designed the study, provided supervision and guidance throughout  
511 the project, and contributed to the writing and revision of the manuscript. All authors contributed to the conception of the study and  
512 participated in the writing and revision of the manuscript.

513  
514  
515  
516 *Competing interests.* The authors declare that they have no known competing financial interests or personal relationships that could  
517 have appeared to influence the work reported in this paper. One of the authors, CRL, serves as an Associate Editor for Biogeosciences.

518  
519  
520  
521 *Acknowledgements.* This work was supported by the Velux Foundation (grant no.29411 to Carolin R. Löscher) and through the DFF  
522 grant from the the Independent Research Fund Denmark (grant no. 0217-00089B to Lasse Riemann, Carolin R. Löscher and Stiig  
523 Markager). ELP was supported by a postdoctoral contract from Danmarks Frie Forskningsfond (DFF, 1026-00428B) at SDU, and by a  
524 Marie Skłodowska- Curie postdoctoral fellowship (HORIZON291 MSCA-2021-PF-01, project number: 101066750) by the European  
525 Commission at Princeton University. We sincerely thank the captain and crew of the P540 during the cruise on the Danish military vessel  
526 for their invaluable support and cooperation at sea. Our gratitude extends to Isaaffik Arctic Gateway for providing the infrastructure and

527 opportunities that made this project possible. We also acknowledge Zarah Kofoed for her technical support in the laboratory and thank all  
528 the Nordceo laboratory technicians for their general assistance.

529 **References**

530

531 Ardyna, M. and Arrigo, K. R.: Phytoplankton dynamics in a changing Arctic Ocean, *Nature Climate Change*, 10, 892–903, 2020.

532 Ardyna, M., Babin, M., Gosselin, M., Devred, E., Rainville, L., and Tremblay, J.-É.: Recent Arctic Ocean sea ice loss triggers novel fall  
533 phytoplankton blooms, *Geophysical Research Letters*, 41, 6207–6212, 2014.

534 Arrigo, K. R. and van Dijken, G. L.: Continued increases in Arctic Ocean primary production, *Progress in oceanography*, 136, 60–70,  
535 2015. Arrigo, K. R., van Dijken, G., and Pabi, S.: Impact of a shrinking Arctic ice cover on marine primary production, *Geophysical*  
536 *Research Letters*, 35, 2008.

537

538 Arrigo, K. R., van Dijken, G. L., Castelao, R. M., Luo, H., Rennermalm, Å. K., Tedesco, M., Mote, T. L., Oliver, H., and Yager, P. L.:  
539 Melting glaciers stimulate large summer phytoplankton blooms in southwest Greenland waters, *Geophysical Research Letters*, 44,  
540 6278– 6285, 2017.

541 Bhatia, M. P., Kujawinski, E. B., Das, S. B., Breier, C. F., Henderson, P. B., and Charette, M. A.: Greenland meltwater as a significant  
542 and potentially bioavailable source of iron to the ocean, *Nature Geoscience*, 6, 274–278, 2013.

543 Blais, M., Tremblay, J.-É., Jungblut, A. D., Gagnon, J., Martin, J., Thaler, M., and Lovejoy, C.: Nitrogen fixation and identification of  
544 potential diazotrophs in the Canadian Arctic, *Global Biogeochemical Cycles*, 26, 2012.

545 Bonnet, S., Biegala, I. C., Dutrieux, P., Slemons, L. O., and Capone, D. G.: Nitrogen fixation in the western equatorial Pacific: Rates,  
546 diazotrophic cyanobacterial size class distribution, and biogeochemical significance, *Global Biogeochemical Cycles*, 23, 2009.

547 Buchanan, P. J., Chase, Z., Matear, R. J., Phipps, S. J., and Bindoff, N. L.: Marine nitrogen fixers mediate a low latitude pathway for  
548 atmospheric CO<sub>2</sub> drawdown, *Nature Communications*, 10, 4611, 2019.

549 Cantalapiedra, C. P., Hernández-Plaza, A., Letunic, I., Bork, P., and Huerta-Cepas, J.: eggNOG-mapper v2: functional annotation,  
550 orthology assignments, and domain prediction at the metagenomic scale, *Molecular biology and evolution*, 38, 5825–5829, 2021.

551 Capone, D. G. and Carpenter, E. J.: Nitrogen fixation in the marine environment, *Science*, 217, 1140–1142, 1982.

552 Chen, Y., Chen, Y., Shi, C., Huang, Z., Zhang, Y., Li, S., Li, Y., Ye, J., Yu, C., Li, Z., et al.: SOAPnuke: a MapReduce acceleration-  
553 supported software for integrated quality control and preprocessing of high-throughput sequencing data, *Gigascience*, 7, gix120, 2018.

554 Cheung, S., Liu, K., Turk-Kubo, K. A., Nishioka, J., Suzuki, K., Landry, M. R., Zehr, J. P., Leung, S., Deng, L., and Liu, H.: High  
555 biomass turnover rates of endosymbiotic nitrogen-fixing cyanobacteria in the western Bering Sea, *Limnology and Oceanography*  
556 Letters

557 Letters, 7, 501–509, 2022.

558 Coale, T. H., Loconte, V., Turk-Kubo, K. A., Vanslembrouck, B., Mak, W. K. E., Cheung, S., Ekman, A., Chen, J.-H., Hagino, K.,  
559 Takano, Y., et al.: Nitrogen-fixing organelle in a marine alga, *Science*, 384, 217–222, 2024.

560 Dähnke, K. and Thamdrup, B.: Nitrogen isotope dynamics and fractionation during sedimentary denitrification in Boknis Eck, Baltic  
561 Sea, *Biogeosciences*, 10, 3079–3088, 2013.

562 Damm, E., Helmke, E., Thoms, S., Schauer, U., Nöthig, E., Bakker, K., and Kiene, R.: Methane production in aerobic oligotrophic  
563 surface water in the central Arctic Ocean, *Biogeosciences*, 7, 1099–1108, 2010.

564 Díez, B., Bergman, B., Pedrós-Alió, C., Antó, M., and Snoeijs, P.: High cyanobacterial *nifH* gene diversity in Arctic seawater and sea  
ice brine, *Environmental microbiology reports*, 4, 360–366, 2012.

565 Emeis, K.-C., Mara, P., Schlarbaum, T., Möbius, J., Dähnke, K., Struck, U., Mihalopoulos, N., and Krom, M.: External N inputs and  
566 internal N cycling traced by isotope ratios of nitrate, dissolved reduced nitrogen, and particulate nitrogen in the eastern Mediterranean  
567 Sea, *Journal of Geophysical Research: Biogeosciences*, 115, 2010.

568 Falkowski, P. G., Fenchel, T., and Delong, E. F.: The microbial engines that drive Earth's biogeochemical cycles, *science*, 320, 1034–  
569 1039, 2008.

570 Farnelid, H., Andersson, A. F., Bertilsson, S., Al-Soud, W. A., Hansen, L. H., Sørensen, S., Steward, G. F., Hagström, Å., and Riemann,  
571 L.: Nitrogenase gene amplicons from global marine surface waters are dominated by genes of non-cyanobacteria, *PloS one*, 6, e19 223,  
572 2011.

573 Farnelid, H., Turk-Kubo, K., Ploug, H., Ossolinski, J. E., Collins, J. R., Van Mooy, B. A., and Zehr, J. P.: Diverse diazotrophs are present  
574 on sinking particles in the North Pacific Subtropical Gyre, *The ISME journal*, 13, 170–182, 2019.

575 Fernández-Méndez, M., Turk-Kubo, K. A., Buttigieg, P. L., Rapp, J. Z., Krumpen, T., and Zehr, J. P.: Diazotroph diversity in the sea ice,  
576 melt ponds, and surface waters of the Eurasian Basin of the Central Arctic Ocean, *Frontiers in microbiology*, 7, 217 140, 2016.

577 Foster, R. A., Goebel, N. L., & Zehr, J. P.: Isolation of calothrix rhizosoleniae (cyanobacteria) strain SC01 from chaetoceros  
578 (bacillariophyta) spp. diatoms of the subtropical north pacific ocean 1. *Journal of Phycology*, 46(5), 1028-1037, 2010.

579 Foster, R. A., Kuypers, M. M., Vagner, T., Paerl, R. W., Musat, N., and Zehr, J. P.: Nitrogen fixation and transfer in open ocean  
580 diatom–cyanobacterial symbioses, *The ISME journal*, 5, 1484–1493, 2011.

581 Foster, R. A., Tienken, D., Littmann, S., Whitehouse, M. J., Kuypers, M. M., and White, A. E.: The rate and fate of N<sub>2</sub> and C fixation  
582 by marine diatom-diazotroph symbioses, *The ISME journal*, 16, 477–487, 2022.

583 Fox, A. and Walker, B. D.: Sources and Cycling of Particulate Organic Matter in Baffin Bay: A Multi-Isotope  $\delta^{13}\text{C}$ ,  $\delta^{15}\text{N}$ , and  $\Delta^{14}\text{C}$   
584 Approach, *Frontiers in Marine Science*, 9, 846 025, 2022.

585 Fu, L., Niu, B., Zhu, Z., Wu, S., and Cd-hit, W. L.: Accelerated for clustering the next-generation sequencing data, *Bioinformatics*,  
586 28, 3150–3152, 2012.

587 Galloway, J., Dentener, F., Capone, D., Boyer, E., Howarth, R., Seitzinger, S., Asner, G., Cleveland, C., Green, P., Holland, E., et al.:  
588 Nitrogen cycles: past, present, and future. *Biogeochemistry* 70, 153e226, 2004.

589 García-Robledo, E., Corzo, A., and Papaspyrou, S.: A fast and direct spectrophotometric method for the sequential determination of  
590 nitrate and nitrite at low concentrations in small volumes, *Marine Chemistry*, 162, 30–36, 2014.

591 Geider, R. J., & La Roche, J.: Redfield revisited: variability of C [ratio] N [ratio] P in marine microalgae and its biochemical  
592 basis. *European Journal of Phycology*, 37(1), 1-17, 2002.

593 Gladish, C. V., Holland, D. M., and Lee, C. M.: Oceanic boundary conditions for Jakobshavn Glacier. Part II: Provenance and sources  
594 of variability of Disko Bay and Ilulissat icefjord waters, 1990–2011, *Journal of Physical Oceanography*, 45, 33–63, 2015.

595 Grosse, J., Bombar, D., Doan, H. N., Nguyen, L. N., & Voss, M.: The Mekong River plume fuels nitrogen fixation and determines  
596 phytoplankton species distribution in the South China Sea during low and high discharge season. *Limnology and  
597 Oceanography*, 55(4), 1668-1680, 2010.

598 Großkopf, T., Mohr, W., Baustian, T., Schunck, H., Gill, D., Kuypers, M. M., Lavik, G., Schmitz, R. A., Wallace, D. W., and LaRoche,  
599 J.: Doubling of marine dinitrogen-fixation rates based on direct measurements, *Nature*, 488, 361–364, 2012.

600 Gruber, N.: The dynamics of the marine nitrogen cycle and its influence on atmospheric CO<sub>2</sub> variations, in: *The ocean carbon cycle  
601 and climate*, pp. 97–148, Springer, 2004.

602 Gruber, N. and Galloway, J. N.: An Earth-system perspective of the global nitrogen cycle, *Nature*, 451, 293–296, 2008.

603 Gruber, N. and Sarmiento, J. L.: Global patterns of marine nitrogen fixation and denitrification, *Global biogeochemical cycles*, 11, 235–  
604 266, 1997.

605 Haine, T. W., Curry, B., Gerdes, R., Hansen, E., Karcher, M., Lee, C., Rudels, B., Spreen, G., de Steur, L., Stewart, K. D., et al.: Arctic  
606 freshwater export: Status, mechanisms, and prospects, *Global and Planetary Change*, 125, 13–35, 2015.

607 Hanna, E., Huybrechts, P., Steffen, K., Cappelen, J., Huff, R., Shuman, C., Irvine-Fynn, T., Wise, S., and Griffiths, M.: Increased runoff  
608 from melt from the Greenland Ice Sheet: a response to global warming, *Journal of Climate*, 21, 331–341, 2008.

609 Hansen, M. O., Nielsen, T. G., Stedmon, C. A., and Munk, P.: Oceanographic regime shift during 1997 in Disko Bay, western  
610 Greenland, *Limnology and Oceanography*, 57, 634–644, 2012.

611 Harding, K., Turk-Kubo, K. A., Sipler, R. E., Mills, M. M., Bronk, D. A., and Zehr, J. P.: Symbiotic unicellular cyanobacteria fix nitrogen  
612 in the Arctic Ocean, *Proceedings of the National Academy of Sciences*, 115, 13 371–13 375, 2018.

613 Hawkings, J., Wadham, J., Tranter, M., Lawson, E., Sole, A., Cowton, T., Tedstone, A., Bartholomew, I., Nienow, P., Chandler, D., et  
614 al.: The effect of warming climate on nutrient and solute export from the Greenland Ice Sheet, *Geochemical Perspectives Letters*, pp.  
615 94–104, 2015.

616 Hawkings, J. R., Wadham, J. L., Tranter, M., Raiswell, R., Benning, L. G., Statham, P. J., Tedstone, A., Nienow, P., Lee, K., and Telling,  
617 J.: Ice sheets as a significant source of highly reactive nanoparticulate iron to the oceans, *Nature communications*, 5, 1–8, 2014.

618 Hendry, K. R., Huvenne, V. A., Robinson, L. F., Annett, A., Badger, M., Jacobel, A. W., Ng, H. C., Opher, J., Pickering, R. A., Taylor, M.  
619 L., et al.: The biogeochemical impact of glacial meltwater from Southwest Greenland, *Progress in Oceanography*, 176, 102 126, 2019.

620 Holland, D. M., Thomas, R. H., De Young, B., Ribergaard, M. H., and Lyberth, B.: Acceleration of Jakobshavn Isbræ triggered by warm  
621 subsurface ocean waters, *Nature geoscience*, 1, 659–664, 2008.

622 Hopwood, M. J., Connelly, D. P., Arendt, K. E., Juul-Pedersen, T., Stinchcombe, M. C., Meire, L., Esposito, M., and Krishna, R.:  
623 Seasonal changes in Fe along a glaciated Greenlandic fjord, *Frontiers in Earth Science*, 4, 15, 2016.

624 Hyatt, D., Chen, G.-L., LoCascio, P. F., Land, M. L., Larimer, F. W., and Hauser, L. J.: Prodigal: prokaryotic gene recognition and  
625 translation initiation site identification, *BMC bioinformatics*, 11, 1–11, 2010.

626 Jensen, H. M., Pedersen, L., Burmeister, A., and Winding Hansen, B.: Pelagic primary production during summer along 65 to 72 N off  
627 West Greenland, *Polar Biology*, 21, 269–278, 1999.

628 Karl, D., Michaels, A., Bergman, B., Capone, D., Carpenter, E., Letelier, R., Lipschultz, F., Paerl, H., Sigman, D., and Stal, L.: Dinitrogen  
629 fixation in the world's oceans, *The nitrogen cycle at regional to global scales*, pp. 47–98, 2002.

630 Knies, J.: Nitrogen isotope evidence for changing Arctic Ocean ventilation regimes during the Cenozoic, *Geophysical Research Letters*,  
631 49, e2022GL099 512, 2022.

632 Krawczyk, D. W., Yesson, C., Knutz, P., Arboe, N. H., Blicher, M. E., Zingler, K. B., and Wagnholt, J. N.: Seafloor habitats across  
633 geological boundaries in Disko Bay, central West Greenland, *Estuarine, Coastal and Shelf Science*, 278, 108 087, 2022.

634 Krupke, A., Mohr, W., LaRoche, J., Fuchs, B. M., Amann, R. I., and Kuypers, M. M.: The effect of nutrients on carbon and nitrogen  
635 fixation by the UCYN-A–haptophyte symbiosis, *The ISME journal*, 9, 1635–1647, 2015.

636 Laso Perez, R., Rivas Santisteban, J., Fernandez-Gonzalez, N., Mundy, C. J., Tamames, J., and Pedros-Alio, C.: Nitrogen cycling during  
637 an Arctic bloom: from chemolithotrophy to nitrogen assimilation, *bioRxiv*, pp. 2024–02, 2024.

638 Lewis, K., Van Dijken, G., and Arrigo, K. R.: Changes in phytoplankton concentration now drive increased Arctic Ocean primary

639 production, *Science*, 369, 198–202, 2020.

640 Li, D., Liu, C.-M., Luo, R., Sadakane, K., and Lam, T.-W.: MEGAHIT: an ultra-fast single-node solution for large and complex  
641 metagenomics assembly via succinct de Bruijn graph, *Bioinformatics*, 31, 1674–1676, 2015.

642 Löscher, C. R., Bourbonnais, A., Dekaezemacker, J., Charoenpong, C. N., Altabet, M. A., Bange, H. W., Czeschel, R., Hoffmann, C.,  
643 and Schmitz, R.: N<sub>2</sub> fixation in eddies of the eastern tropical South Pacific Ocean, *Biogeosciences*, 13, 2889–2899, 2016.

644 Löscher, C. R., Mohr, W., Bange, H. W., and Canfield, D. E.: No nitrogen fixation in the Bay of Bengal?, *Biogeosciences*, 17, 851–864,  
645 2020. Luo, Y.-W., Doney, S., Anderson, L., Benavides, M., Berman-Frank, I., Bode, A., Bonnet, S., Boström, K. H., Böttjer, D., Capone,  
646 D., et al.: Database of diazotrophs in global ocean: abundance, biomass and nitrogen fixation rates, *Earth System Science Data*, 4, 47–73,  
647 2012.

648 Martínez-Pérez, C., Mohr, W., Löscher, C. R., Dekaezemacker, J., Littmann, S., Yilmaz, P., Lehnen, N., Fuchs, B. M., Lavik, G.,  
649 Schmitz,  
650 R. A., et al.: The small unicellular diazotrophic symbiont, UCYN-A, is a key player in the marine nitrogen cycle, *Nature Microbiology*,  
651 1, 1–7, 2016.

652 Mills, M. M., Turk-Kubo, K. A., van Dijken, G. L., Henke, B. A., Harding, K., Wilson, S. T., Arrigo, K. R., and Zehr, J. P.: Unusual  
653 marine cyanobacteria/haptophyte symbiosis relies on N<sub>2</sub> fixation even in N-rich environments, *The ISME Journal*, 14, 2395–2406,  
654 2020.

655 Mohr, W., Grosskopf, T., Wallace, D. W., and LaRoche, J.: Methodological underestimation of oceanic nitrogen fixation rates, *PloS one*,  
656 5, e12 583, 2010.

657 Montoya, J. P.: Nitrogen stable isotopes in marine environments, *Nitrogen in the marine environment*, 2, 1277–1302, 2008.

658 Montoya, J. P., Carpenter, E. J., and Capone, D. G.: Nitrogen fixation and nitrogen isotope abundances in zooplankton of the oligotrophic  
659 North Atlantic, *Limnology and Oceanography*, 47, 1617–1628, 2002.

660 Mortensen, J., Rysgaard, S., Winding, M., Juul-Pedersen, T., Arendt, K., Lund, H., Stuart-Lee, A., and Meire, L.: Multidecadal water  
661 mass dynamics on the West Greenland Shelf, *Journal of Geophysical Research: Oceans*, 127, e2022JC018 724, 2022.

662 Munk, P., Nielsen, T. G., and Hansen, B. W.: Horizontal and vertical dynamics of zooplankton and larval fish communities during mid-  
663 summer in Disko Bay, West Greenland, *Journal of Plankton Research*, 37, 554–570, 2015.

664 Murphy, J. and Riley, J. P.: A modified single solution method for the determination of phosphate in natural waters, *Analytica chimica  
665 acta*, 27, 31–36, 1962.

666 Myers, P. G. and Ribergaard, M. H.: Warming of the polar water layer in Disko Bay and potential impact on Jakobshavn Isbrae, *Journal  
667 of Physical Oceanography*, 43, 2629–2640, 2013.

668 Patro, R., Duggal, G., Love, M. I., Irizarry, R. A., and Kingsford, C.: Salmon provides fast and bias-aware quantification of transcript  
669 expression, *Nature methods*, 14, 417–419, 2017.

670 Quigg, A., Finkel, Z.V., Irwin, A.J., Rosenthal, Y., Ho, T.Y., Reinfelder, J.R., Schofield, O., Morel, F.M. and Falkowski, P.G.: The  
671 evolutionary inheritance of elemental stoichiometry in marine phytoplankton. *Nature*, 425(6955), pp.291-294, 2003.

672 Redfield, A. C.: On the proportions of organic derivatives in sea water and their relation to the composition of plankton (Vol. 1). Liverpool:  
673 university press of liverpool, 1934.

674 Reeder, C. F., Stoltenberg, I., Javidpour, J., and Löscher, C. R.: Salinity as a key control on the diazotrophic community composition in  
675 the Baltic Sea, *Ocean Science Discussions*, 2021, 1–30, 2021.

676 Rees, A. P., Gilbert, J. A., and Kelly-Gerrey, B. A.: Nitrogen fixation in the western English Channel (NE Atlantic ocean), *Marine*

677 Ecology Progress Series, 374, 7–12, 2009.

678 Rysgaard, S., Boone, W., Carlson, D., Sejr, M., Bendtsen, J., Juul-Pedersen, T., Lund, H., Meire, L., and Mortensen, J.: An updated view  
679 on water masses on the pan-west Greenland continental shelf and their link to proglacial fjords, *Journal of Geophysical Research: Oceans*, 125, e2019JC015 564, 2020.

680 Schiøtt, S.: The Marine Ecosystem of Ilulissat Icefjord, Greenland, Ph.D. thesis, Department of Biology, Aarhus University, Denmark, 2023. Schlitzer, R.: Ocean data view, 2022.

681 Schneider, B., Schlitzer, R., Fischer, G. and Nöthig, E.M.: Depth-dependent elemental compositions of particulate organic matter (POM) in the ocean. *Global Biogeochemical Cycles*, 17(2), 2003.

682 Schvarcz, C. R., Wilson, S. T., Caffin, M., Stancheva, R., Li, Q., Turk-Kubo, K. A., White, A. E., Karl, D. M., Zehr, J. P., and Steward, G. F.: Overlooked and widespread pennate diatom-diazotroph symbioses in the sea, *Nature communications*, 13, 799, 2022.

683 Shao, Z., Xu, Y., Wang, H., Luo, W., Wang, L., Huang, Y., Agawin, N. S. R., Ahmed, A., Benavides, M., Bentzon-Tilia, M., et al.: Global oceanic diazotroph database version 2 and elevated estimate of global N 2 fixation, *Earth System Science Data*, 15, 2023.

684 Sherwood, O. A., Davin, S. H., Lehmann, N., Buchwald, C., Edinger, E. N., Lehmann, M. F., and Kienast, M.: Stable isotope ratios in seawater nitrate reflect the influence of Pacific water along the northwest Atlantic margin, *Biogeosciences*, 18, 4491–4510, 2021.

685 Shiozaki, T., Bombar, D., Riemann, L., Hashihama, F., Takeda, S., Yamaguchi, T., Ehama, M., Hamasaki, K., and Furuya, K.: Basin scale variability of active diazotrophs and nitrogen fixation in the North Pacific, from the tropics to the subarctic Bering Sea, *Global Biogeochemical Cycles*, 31, 996–1009, 2017.

686 Shiozaki, T., Fujiwara, A., Ijichi, M., Harada, N., Nishino, S., Nishi, S., Nagata, T., and Hamasaki, K.: Diazotroph community structure and the role of nitrogen fixation in the nitrogen cycle in the Chukchi Sea (western Arctic Ocean), *Limnology and Oceanography*, 63, 2191–2205, 2018.

687 Shiozaki, T., Fujiwara, A., Inomura, K., Hirose, Y., Hashihama, F., and Harada, N.: Biological nitrogen fixation detected under Antarctic sea ice, *Nature geoscience*, 13, 729–732, 2020.

688 Shiozaki, T., Nishimura, Y., Yoshizawa, S., Takami, H., Hamasaki, K., Fujiwara, A., Nishino, S., and Harada, N.: Distribution and survival strategies of endemic and cosmopolitan diazotrophs in the Arctic Ocean, *The ISME journal*, 17, 1340–1350, 2023.

689 Sigman, D. M., DiFiore, P. J., Hain, M. P., Deutsch, C., Wang, Y., Karl, D. M., Knapp, A. N., Lehmann, M. F., and Pantoja, S.: The dual isotopes of deep nitrate as a constraint on the cycle and budget of oceanic fixed nitrogen, *Deep Sea Research Part I: Oceanographic Research Papers*, 56, 1419–1439, 2009.

690 Sipler, R. E., Gong, D., Baer, S. E., Sanderson, M. P., Roberts, Q. N., Mulholland, M. R., and Bronk, D. A.: Preliminary estimates of the contribution of Arctic nitrogen fixation to the global nitrogen budget, *Limnology and Oceanography Letters*, 2, 159–166, 2017.

691 Slawyk, G., Collos, Y., and Auclair, J.-C.: The use of the 13C and 15N isotopes for the simultaneous measurement of carbon and nitrogen turnover rates in marine phytoplankton 1, *Limnology and Oceanography*, 22, 925–932, 1977.

692 Sohm, J. A., Webb, E. A., and Capone, D. G.: Emerging patterns of marine nitrogen fixation, *Nature Reviews Microbiology*, 9, 499–508, 2011.

693 Sterner, R. W., & Elser, J. J. Ecological stoichiometry: the biology of elements from molecules to the biosphere. In *Ecological stoichiometry*. Princeton university press, 2017.

694 Tanioka, T., Garcia, C.A., Larkin, A.A., Garcia, N.S., Fagan, A.J. and Martiny, A.C.: Global patterns and predictors of C: N: P in marine ecosystems. *Communications Earth & Environment*, 3(1), p.271, 2022.

714 Tang, W., Wang, S., Fonseca-Batista, D., Dehairs, F., Gifford, S., Gonzalez, A. G., Gallinari, M., Planquette, H., Sarthou, G., and Cassar,  
715 N.: Revisiting the distribution of oceanic N<sub>2</sub> fixation and estimating diazotrophic contribution to marine production, *Nature*  
716 *communications*, 10, 831, 2019.

717 Tremblay, J.-É. and Gagnon, J.: The effects of irradiance and nutrient supply on the productivity of Arctic waters: a perspective on  
718 climate change, in: *Influence of climate change on the changing arctic and sub-arctic conditions*, pp. 73–93, Springer, 2009.

719 Turk, K. A., Rees, A. P., Zehr, J. P., Pereira, N., Swift, P., Shelley, R., Lohan, M., Woodward, E. M. S., and Gilbert, J.: Nitrogen fixation  
720 and nitrogenase (*nifH*) expression in tropical waters of the eastern North Atlantic, *The ISME journal*, 5, 1201–1212, 2011.

721 Turk-Kubo, K. A., Frank, I. E., Hogan, M. E., Desnues, A., Bonnet, S., and Zehr, J. P.: Diazotroph community succession during the  
722 VAHINE mesocosm experiment (New Caledonia lagoon), *Biogeosciences*, 12, 7435–7452, 2015.

723 Von Friesen, L. W. and Riemann, L.: Nitrogen fixation in a changing Arctic Ocean: an overlooked source of nitrogen?, *Frontiers in*  
724 *Microbiology*, 11, 596 426, 2020.

725 Wang, S., Bailey, D., Lindsay, K., Moore, J., and Holland, M.: Impact of sea ice on the marine iron cycle and phytoplankton productivity,  
726 *Biogeosciences*, 11, 4713–4731, 2014.

727 Zehr, J. P. and Capone, D. G.: Changing perspectives in marine nitrogen fixation, *Science*, 368, eaay9514, 2020.